

QUANTITATIVE ^{19}F MR MOLECULAR IMAGING WITH B_1 -MAPPING COMPENSATION

Matthew Goette^{1,2}, Shelton Caruthers¹, Gregory Lanza¹, and Samuel Wickline¹

¹Cardiology, Washington University in St. Louis, St. Louis, MO, United States, ²Pediatric Radiology, Texas Children's Hospital, Houston, TX, United States

Target Audience: Basic researchers interested in quantitative molecular imaging, particularly of targeted contrast agents and non-proton agents, as well as imaging scientists studying applications of B_1 mapping.

Purpose: Quantitative MR molecular imaging allows for the detection of targeted contrast agents to diagnose disease states and monitor response to therapy, such as angiogenic therapy in peripheral vascular disease¹ and anti-angiogenic therapy in atherosclerosis and cancer² with $\alpha_v\beta_3$ -integrin targeted perfluorocarbon (PFC) nanoparticles. Recently, ^{19}F MR using a $^{19}\text{F}/^1\text{H}$ dual-tuned RF coil has been utilized to directly image and quantify the fluorinated core of these PFC nanoparticle (NP) emulsions³. Ultra-short echo time (UTE) balanced steady state free precession (bSSFP) sequences have been shown to be much more sensitive to ^{19}F imaging agents than other techniques⁴. However, low concentrations of these fluorine agents in the body, even in the absence of any physiological background signal, in conjunction with varying RF coil sensitivity profiles (i.e. B_1 -field inhomogeneities) raises obstacles to optimized imaging and accurate quantification⁵. This study presents a strategy to more accurately quantify the sparse ^{19}F signal from PFC NP emulsions with a ^1H image-based actual flip angle (AFI)⁶ B_1 -mapping correction to the ^{19}F and ^1H images with a phantom and an *in vivo* imaging experiment.

Methods: An $\alpha_v\beta_3$ -integrin targeted perfluoro-15-crown-5-ether (PFCE: $\text{C}_{10}\text{F}_{20}\text{O}_5$) nanoparticle emulsion (20 vol%) was prepared as previously published⁷. A phantom was made with two 5 mL glass vials (inner diameter 15 mm) filled with 1.0 M PFCE NP in 2% agar, aligned 2 cm apart in 200 mL bottle of 1.0% saline. In accordance with institution-approved protocols, New Zealand White Rabbits (2 kg, n=3) were implanted with a VX2 adenocarcinoma tumor (2-3 cm) in the hind leg⁸. Angiogenesis imaging was performed 2 weeks post implantation (tumor size ~ 15 mm), under ketamine/xylazine anesthesia, and injected intravenously 3 hours before imaging. MR data were acquired on a 3.0 T clinical whole-body scanner (Achieva, Philips Healthcare, Best, The Netherlands) with a dual $^{19}\text{F}/^1\text{H}$ spectrometer system and a dual-tuned transmit/receive single loop surface RF coil (7×12 cm). A simultaneous $^{19}\text{F}/^1\text{H}$ 3D UTE bSSFP imaging sequence⁴ with Wong-type 3D radial readout trajectory was used for both the phantom and *in vivo* experiment with: 140 mm FOV, matrix 64³, isotropic voxel $\Delta x=2.3$ mm, exBW=4 kHz centered on PFCE peak, pBW=400 Hz, $\alpha=30^\circ$, TR/TE=2.32/0.13 ms, Nyquist radius=0.23, NSA=56, 35 min scan time. The B_1 field was mapped using an actual flip angle imaging (AFI) sequence with: 140 mm FOV, 96² matrix, 15 4-mm slices, 1.4×1.4×0.6 mm resolution, $\alpha = 70^\circ$, 2.8 min scan time. Using the flip angle map [$\text{AFI}=\alpha_{\text{requested}}/\alpha_{\text{nominal}}$] and a model of the bSSFP signal [Eq. 1], a spatially-dependent calibration mask (ρ) was calculated [Eq. 2] in MATLAB (MathWorks, Inc., Natick, MA) and used to compensate the ^1H and ^{19}F signal intensities of the bSSFP molecular imaging sequence by dividing each image by ρ , pixel by pixel. Importantly for the *in vivo* model, the same correction scheme was performed on the imaging slice that contained the fluorine standard (150 mM_{19F}) to which the bound nanoparticle ^{19}F signal was compared for quantitation.

$$\text{bSSFP} = k \sin \alpha \sqrt{E_2} \frac{1-E_1}{1-E_1 E_2 - (E_1 - E_2) \cos \alpha} \quad [\text{Eq. 1}]$$

$$\rho = \text{AFI} * \sin(\text{AFI} * \alpha_{\text{nom}}) \frac{1-E_1}{1-E_1 E_2 - (E_1 - E_2) \cos(\text{AFI} * \alpha_{\text{nom}})} \quad [\text{Eq. 2}]$$

$$E_1 = e^{-\text{TR}/T_1}; E_2 = e^{-\text{TE}/T_2}$$

Results: Figure 1 demonstrates a ^1H -image-based B_1 correction used to equalize the signal intensity of ^{19}F and ^1H images for two identical PFC-NP samples placed in different parts of the RF field. Before correction, the ^{19}F image (Fig. 1a) and $^{19}\text{F}/^1\text{H}$ overlay image (Fig. 1b) exhibit the effects of the inhomogeneous RF field produced by the surface coil. Mean signal intensity in the vial closest to the coil was 2537 ± 176 arbitrary units (a.u.), while the ^{19}F signal from the identical vial 2 cm farther from the coil was 66.0% lower (863 ± 40 a.u., $p < 0.001$). The B_1 -field was mapped using the ^1H signal with actual flip angle imaging (% actual/requested FA) (Fig. 1c), and input into Eq. 2 to create a correction ratio (Fig. 1d). This factor was used to correct both ^{19}F and ^1H signal intensities, as displayed in Figure 1e&f. After correction, the mean signal intensity in the vial closest to the coil (2621 ± 156 a.u.) was not significantly different ($p = 0.85$) than that in the vial farther from the coil (2681 ± 129 a.u.). The same correction method yielded a 27.5% increase ($p < 0.05$) in ^{19}F signal from PFC-NP that were targeted to $\alpha_v\beta_3$ -integrins in rabbit tumor neovasculature (before: 20.0 ± 0.12 mM_{19F}, after: 25.5 ± 0.10 mM_{19F}), as shown in Figure 2.

Discussion and Conclusion: An image-based B_1 -mapping correction can be used to correct signal intensities for simultaneously acquired ^1H and ^{19}F images of angiogenesis in a phantom and an *in vivo* rabbit model. This technique results in a more homogeneous ^1H image of the anatomy and facilitates measurement of bound $\alpha_v\beta_3$ -integrin targeted nanoparticles with ^{19}F imaging, correcting for known B_1 inhomogeneities. Correction techniques such as this one are required to improve accuracy and repeatability of measurements of molecular imaging agents in preclinical and clinical trials, thereby facilitating translation of molecular imaging, and in particular ^{19}F imaging using fluorinated nanoparticles, into the clinic.

References: ¹Winter, et al. Magn Reson Med. 2010;64:369-376. ²Lanza, et al. Eur J Nucl Med Mol Img. 2010;37: S114-S126. ³Caruthers, et al. MedicaMundi. 2010;54(2): 5-13. ⁴Keupp, et al. Proc Int'l Soc Mag Reson Med 18. 2010. ⁵Goette, et al. Magn Reson Med. 2014; doi: 10.1002/mrm.25437. ⁶Yarnykh. Magn Reson Med. 2007;57(1):192-200. ⁷Keupp, et al. Mag Reson Med. 2011;66(4): 1116-1122. ⁸Hu, et al. Int J Cancer. 2007;120(9):1951-1957.

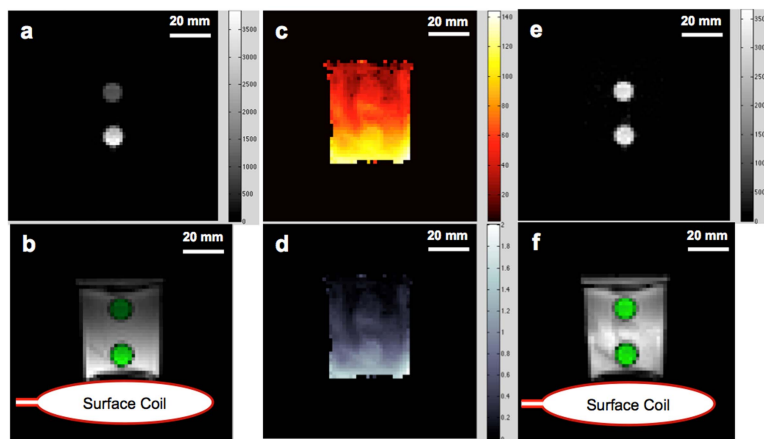


Figure 1. ^{19}F MRI of phantom with two vials of 1.0 M PFC-NP in agar using a simultaneous $^{19}\text{F}/^1\text{H}$ UTE-bSSFP sequence and a $^{19}\text{F}/^1\text{H}$ dual-tuned surface coil. ^1H -image-based B_1 correction equalized the signal intensity of ^{19}F images the two samples, which were offset significantly by ~66% ($p < 0.001$) before correction.

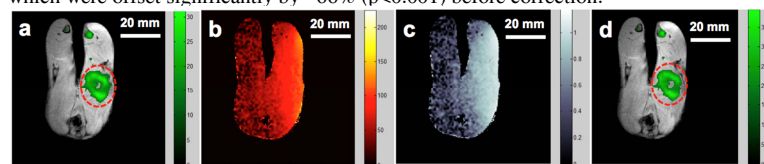


Figure 2. B_1 -mapping compensation of *in vivo* cancer model in rabbit with the use of $\alpha_v\beta_3$ -integrin-targeted PFC NP nanoparticles captured by ^{19}F MRI with a $^{19}\text{F}/^1\text{H}$ dual-tuned surface coil (located at image right). In the uncorrected ^{19}F image overlaid on the high-resolution ^1H image (a), PFC NP concentration was quantified as 20.0 ± 0.12 mM_{19F}. B_1 -field mapping with AFI (% actual/requested FA) (b) and calibration mask calculated from a UTE-bSSFP signal model (c). In the corrected ^{19}F image overlaid on the high-resolution ^1H image (d), PFC NP concentration was quantified as 25.5 ± 0.10 mM_{19F}.